Archives of Civil and Mechanical Engineering (2020) 20:32
https://doi.org/10.1007/s43452-019-0006-8

ORIGINAL ARTICLE

Investigation on self-healing of neat and polymer modified asphalt binders

C. Wang[1] · L. Xue[1] · W. Xie[1] · W. Cao[2]

Received: 1 July 2019 / Accepted: 12 November 2019 / Published online: 6 March 2020

Abstract
The paving asphalts have long been recognized to be capable of self-healing. The objective of this study was to evaluate the healing potential of asphalt binders and investigate its relationship with molecular characteristics in terms of composition and structures. Five neat and styrene–butadiene–styrene (SBS) modified asphalt binders were characterized using the recently developed linear amplitude sweep-based healing test. The data were analyzed based on the viscoelastic continuum damage theory to establish healing master curves and determine the healing rate H^R. Chemical evaluation methods included saturates, aromatics, resins, and asphaltenes fractionation, gel permeation chromatography, and nuclear magnetic resonance spectroscopy. Results indicated that the presence of more light/low-polarity fractions of saturates and aromatics or higher concentrations of small molecules promoted healing, as these molecules were expected to have higher mobility facilitating molecular diffusion across crack interfaces. Lower percentages of aromatic ring structures and more aliphatic chains corresponded to higher healing rates. The SBS-modified asphalt binders contained higher concentrations of aromatic rings, but still provided comparable healing potential with the neat asphalts.

Keywords Asphalt binder · Self-healing · Polymer · Molecular characteristics · Viscoelastic continuum damage theory

1 Introduction

Fatigue cracking is one of the primary concerns regarding the durability of flexible pavement. Crack may initiate at the bottom of the asphalt layer due to tensile stress or beneath the tire due to shearing and propagate through the layer under repeated traffic loading. A number of test methods has been developed and implemented in the past decades for evaluating the fatigue resistance of asphalt concrete [1, 2], including the well-known four-point bending beam fatigue test. Meanwhile, it has also been widely recognized that there exists a pronounced discrepancy between the laboratory and field measured fatigue lives. This difference can be primarily attributed to the fact that the wheel loading is not continuous but intermittent, allowing partial recovery of materials' integrity, which is referred to as self-healing. As fatigue damage typically occurs during the intermediate temperature region, elevated temperatures during summer months present another contributing factor by promoting the self-healing process [3]. To bridge the gap between laboratory and field fatigue performance, a calibration factor for the beam fatigue test typically in the range of 6–70 or even higher is called for [4].

The cohesive healing of asphalt plays a significant role in the macroscopic healing phenomenon of asphalt mixtures. One understanding of the healing mechanism borrowed from Wool and O'Connor's healing theory for polymers considers that healing has two processes: wetting and intrinsic healing [5–7]. The latter process is further comprised of two mechanisms of different time scales: the instantaneous interfacial cohesion and molecular diffusion across the interface that occurs in the long term. Therefore, small molecules with weak or no polarity are expected to diffuse easily, thereby facilitating the healing process. Sun et al. [8] found that asphalt self-healing was more sensitive to the contents of aromatics (with the smallest molecular weight of the four components) and small molecules than other fractions or molecular sizes. On the other hand, Santagata et al. [9]

✉ W. Cao
WeiCao5980@gmail.com

[1] Department of Road and Railway Engineering, Beijing University of Technology, Beijing, People's Republic of China

[2] Department of Civil Engineering, Central South University, Changsha, Hunan, People's Republic of China

proposed to use the ratio of saturates to aromatics (S/Ar) and believed that a higher S/Ar represents an overall longer and thinner molecular structure of asphalt, which provides lower hindrance when molecules diffuse. The S/Ar ratio has been found to be positively correlated with the healing potential of asphalts [8, 9]. Kim et al. [10] proposed to use the ratio of methylene to methyl functional groups as an indicator of the concentration of long-chained aliphatic molecules and side chains. They reported that asphalt healing was promoted with increase in this ratio. Another school of thought considers asphalt as a complex blend of molecules, in which the polar molecules are dispersed and the nonpolar ones form the polar–polar associations [11]. These weak bonds are constantly breaking and reforming due to disturbance in the mechanical and thermodynamic states. With the new bonds established, self-healing is exhibited on the macroscopic level.

Given the complexity of the underlying mechanism, a variety of experimental methods have been developed to practically capture the healing effect and various phenomenological indices proposed to quantify it. Basin et al. [6] proposed to use dynamic shear rheometer (DSR) and a two-piece specimen setup to investigate asphalt self-healing. They brought two disk specimens into contact between the DSR end plates and applied a few small-strain oscillations at various time intervals for monitoring the stiffness, which was then used to quantify the intrinsic healing. Santagata et al. [9] introduced a 2-h rest period into the otherwise continuous (stress-controlled) time sweep test in a DSR and monitored the stiffness recovery during the rest period using small-strain oscillations. They developed a healing index based on the observation that the second loading phase yielded a stiffness evolution time history that followed the trend of the first phase. Sun et al. [8] adopted a similar approach by inserting a 1-h rest into the strain-controlled time sweep test and proposed an alternative healing index based on the initial stiffness and the stiffness values immediately before and after the rest period. Lv et al. [3] utilized the binder bond strength (BBS) test for which the healing was accomplished by submerging the whole setup in a 25 °C water bath for 24 h; the healing index was defined as the ratio of the pull-off tensile strength after healing cycles to the initial strength. Xie et al. [12, 13] developed the linear amplitude sweep-based healing (LASH) test by inserting a rest period into the linear amplitude sweep (LAS) test (an accelerated fatigue protocol as compared to time sweep). Advanced analysis based on the viscoelastic continuum damage (VECD) theory provided the damage intensities immediately before and after the rest period, which were employed to define the healing index.

The LASH test was adopted in the present study for characterizing the healing potential of asphalt binders. This test was selected considering that the healing index was determined based on the damage reversal, which is believed more essentially related to self-healing than the use of gains in stiffness or load cycles. The objective was to investigate the relationship between the phenomenological healing potential and the molecular characteristics of asphalt binders. For this purpose, the following chemical evaluations were performed: saturates, aromatics, resins, and asphaltenes (SARA) fractionation, gel permeation chromatography (GPC) for molecular weight/size distribution, and nuclear magnetic resonance (NMR) spectroscopy for molecular structures.

2 Materials and methodologies

2.1 Asphalt materials

Three neat asphalts with different penetration grades along with two styrene–butadiene–styrene (SBS) modified binders were employed in this study. Table 1 presents the physical properties of the asphalt binders at the virgin state in terms of the Superpave performance grade (PG), penetration, softening point, and ductility. Prior to testing, all asphalt binders were subjected to the rolling thin-film oven (RTFO) test [14] to simulate the short-term aging effects induced during the mixture production and placement processes.

Table 1 Asphalt binder designation and physical properties

Asphalt binders	Designation	PG	Modification	Penetration (0.1 mm, 25 °C)	Softening point (°C)	Ductility (mm, 10 °C)
Neat	N-30	82-16	–	22.2	61.1	–
	N-50	70-22	–	51.9	52.7	11.9
	N-70	64-22	–	71.5	48.4	37.3
SBS modified	SBS-A	82-22	4% SBS linear	63.4	72.7	48.7
	SBS-B	82-28	4.5% SBS linear	62.6	75.5	47.9

PG performance grade

2.2 LASH test

The healing characterization methodology consisted of LAS and LASH tests. The LAS test is a well-established accelerated fatigue assessment protocol for asphalt binders [15]. This test employs a continuous strain-controlled oscillation in a DSR with the strain amplitude linearly increasing from 0.1 to 30% over 3000 cycles. The LASH test was adapted from the LAS test by inserting a rest period of various durations into its loading profile [12]. The rest period can be applied at any damage state of the test sample. Figure 1 illustrates the sample preparation and setup and the fracture surface exposed by raising the DSR spindle after the test. As shown in Fig. 1c, fatigue damage was manifested as hairline cracks propagating from sample periphery to the center. Table 2 presents the testing matrix for the LASH test, which included four different rest periods each applied at four different damage levels. In this study, both LAS and LASH tests were performed using an Anton Paar MCR 302 DSR equipment with 8-mm diameter and 2-mm gap parallel plates setup. All tests were conducted at a frequency of 10 Hz and an intermediate temperature of 20 °C. A minimum of two replicates were utilized in each case and the discrepancy in the time history of the stiffness among the replicates was minimal.

2.3 SARA fractionation

Asphalt binder can be divided based on its pentane or heptane solubility into asphaltenes and maltenes, while maltenes can be further separated into saturates, aromatics, and resins. Asphaltenes are the highly polar component featuring a higher hardness and brittleness compared to the other fractions. As such, asphaltenes play a significant role in the rheological properties (viscosity) of asphalt binders [16]. Resins consist of molecules that are smaller and less polar than asphaltenes and have a considerable influence on the temperature sensitivity of viscosity [17]. The aromatics-containing aromatic rings are slightly polarizable, whereas the saturates are nonpolar consisting of linear, branched, and cyclic hydrocarbons. In this study, for each asphalt binder, the asphaltenes fraction was initially precipitated using *n*-heptane. The remaining maltenes component was then separated into the other three fractions using the thin layer chromatography according to ASTM D4124 [18].

Table 2 Testing matrix for the LASH test

Damage level	Rest periods
25% S_f	60 s, 300 s, 900 s, 1800 s
50% S_f	60 s, 300 s, 900 s, 1800 s
75% S_f	60 s, 300 s, 900 s, 1800 s
125% S_f	60 s, 300 s, 900 s, 1800 s

S_f damage level at fatigue failure identified from the LAS test

2.4 GPC test

Compared to the SARA fractionation, the GPC test provides an alternative approach for component separation based on the sizes (hydrodynamic volumes) of different molecules. The process is in principle similar to aggregate sieving, in which the largest molecules elute first, followed by the smaller ones. The resultant chromatogram is typically divided into three portions [19]: large molecular size (LMS), medium molecular size (MMS), and small molecular size (SMS). Asphalt binders with identical molecular weight/size distributions are anticipated to exhibit similar rheological behaviors [20]. In this study, the GPC test was conducted in a Waters GPC system equipped with Waters 2410 differential refractive index detector. Tetrahydrofuran (THF) was used as the solvent at a flow rate of 1 mL/min. Each asphalt binder was dissolved at a concentration of 0.25% in the solvent. The 0.45 µm Teflon filters were used for prefiltration of the obtained solution.

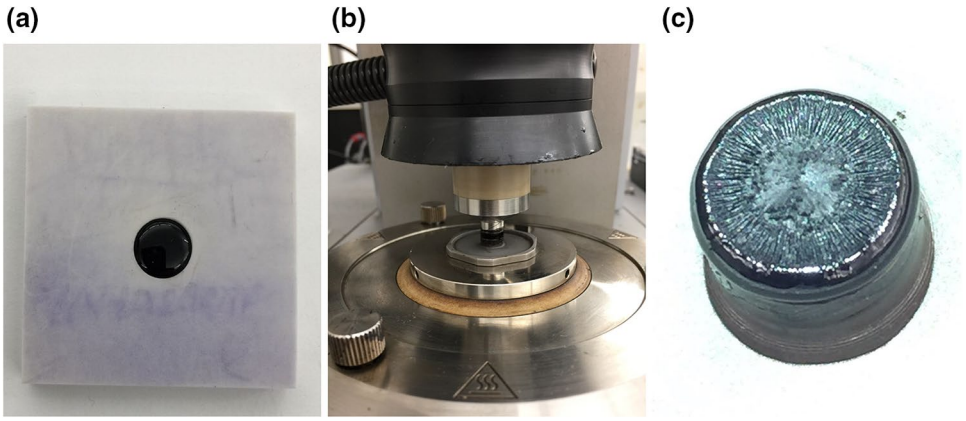

Fig. 1 The LASH test: **a** sample prepared in silicone mold, **b** sample setup in DSR, and **c** fracture surface featuring radial hairline cracks

2.5 NMR test

Since asphalt binder is such an extremely complex substance, a complete separation and identification of all the compounds in it is not practically feasible. The ^{1}H NMR spectroscopy provides insights into the averaged molecular structure, as different chemical environment of the hydrogen molecules can be revealed by the chemical shift of the resonance peaks in the obtained spectrum [8, 21]. In this study, a Bruker AVANCE HD III 400 MHz spectrometer was utilized to measure the ^{1}H NMR spectra of the asphalt binders. The percentages of aromatic and aliphatic hydrogens were determined using the software MestReNova based on the resonance peaks.

3 Healing characterization results

This section presents the results of healing characterization, including the damage characteristic relationships, healing master curves, and two healing parameters, namely healing percentage and healing rate.

3.1 Healing percentage

By applying the VECD theory, the LAS and LASH data can be processed to yield a function referred to as the damage characteristic relationship [12, 13, 15], which correlates material structural integrity (C) and an internal state variable for damage intensity (S). The following outline the incremental form for the calculation of S per cycle:

$$\Delta C_i = C_i - C_{i-1}, \tag{1}$$

where C_i is the normalized dynamic shear modulus (representing material integrity) of the ith cycle; ΔC and ΔS are the increments in C and S per cycle, respectively; DMR stands for dynamic modulus ratio accounting for specimen-to-specimen variability; $\gamma_{pp,i}$ is the peak-to-peak strain amplitude of the ith cycle; $|G^*|_{LVE}$ is the linear viscoelastic dynamic shear modulus of the material at the test condition; α is damage evolution rate; and Δt is the time difference between the strain peaks in the i- and $(i-1)$-th cycles. More detailed description of the analysis can be found in the literature [22–24].

In the LAS test, due to continuous loading, the specimen was constantly losing its structural integrity, i.e., $\Delta C < 0$, thereby yielding a monotonically decreasing $C(S)$ curve; see the solid lines in Fig. 2. In the LASH test, however, the specimen experienced a partial recovery of its integrity right after the rest as evidenced by a positive ΔC. Using the corresponding algorithm in Eq. (2), damage reversal (i.e., $\Delta S < 0$) was achieved which mathematically describes the healing occurrence. Graphically, the combination of positive ΔC and negative ΔS presents a broken $C(S)$ curve that is shifted toward the upper-left corner after the rest; see the symbols in Fig. 2. Note that the $C(S)$ relation obtained from the LAS test is a unique material function, independent of test conditions (temperature, frequency) and mode of loading [23, 24]. However, once significant healing is present as in the LASH test by introducing the rest period, this uniqueness feature is lost. Various rest periods applied at different damage levels would result in different $C(S)$ curve segments right after the rest, exhibiting a shift relative to the segment before the rest. The LAS-based continuous $C(S)$ curve was set as the reference and the amount of shift with respect to it

$$\begin{cases} \text{For } \Delta C_i < 0\text{: } \Delta S_i = \left[\frac{1}{2}\text{DMR}\left(\gamma_{pp,i}\cdot|G*|_{LVE}\right)^2\left(-\Delta C_i\right)\right]^{\frac{\alpha}{1+\alpha}}(\Delta t)^{\frac{1}{1+\alpha}} > 0 \\ \text{For } \Delta C_i > 0\text{: } \Delta S_i = -\left[\frac{1}{2}\text{DMR}\left(\gamma_{pp,i}\cdot|G*|_{LVE}\right)^2\left(\Delta C_i\right)\right]^{\frac{\alpha}{1+\alpha}}(\Delta t)^{\frac{1}{1+\alpha}} < 0, \end{cases} \tag{2}$$

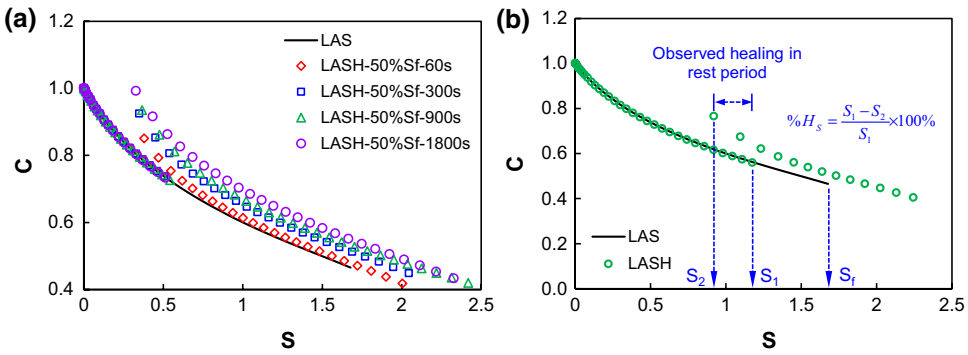

Fig. 2 The LASH test: **a** $C(S)$ curves for the N-70 asphalt binder with the rest periods applied at 50% S_f and **b** illustration of the calculation of healing percentage

was then made use of to quantify the self-healing that had occurred during the rest period:

$$\%H_S = \frac{S_1 - S_2}{S_1} \times 100\%, \tag{3}$$

where $\%H_S$ is healing percentage and S_1 and S_2 are the damage levels right before and after the rest period as shown in Fig. 2b.

Figure 3 presents the $\%H_S$ results for the asphalt binders under different damage levels and rest durations. For a given rest period, the healing percentage reduced considerably, when the rest period was applied at higher damage levels (with the presence of more cracked micro-surfaces). For a given asphalt binder, extending the rest period in general was beneficial to healing by providing higher $\%H_S$ values. The N-70 binder exhibited the highest healing potential at the lowest damage level of 25% S_f, followed by N-50. At the medium damage levels of 50% and 75% S_f, all the five asphalt binders demonstrated similar healing behaviors. When the rest period was applied after fatigue failure at 125% S_f, the N-30 binder lost its healing potential within the 1800 s window, whereas the two SBS-modified binders exhibited the highest healing percentages. Further, use of the additional 0.5% SBS modification in SBS-B appeared to bring about slightly higher $\%H_S$ results. In general, the description of material's mechanical behavior should transition upon fatigue failure from continuum damage mechanics for crack initiation to fracture mechanics for crack propagation. The above observation suggested that the SBS polymer modifier was able to retard the crack propagation, which is consistent with earlier studies [25] and that a fracture mechanics-based methodology is needed to better investigate phenomenologically the effect of SBS modification.

3.2 Healing rate

The healing percentage $\%H_S$ depends on the length of rest period and when the rest is applied. For engineering applications, a single-valued index representing the overall healing potential may be preferred. For this purpose, the healing rate parameter was developed by constructing the so-called healing master curve, a process analogous to construction of the well-known dynamic modulus master curve of asphalt concrete. To do so, the $\%H_S$ results from all damage levels were plotted with respect to rest period

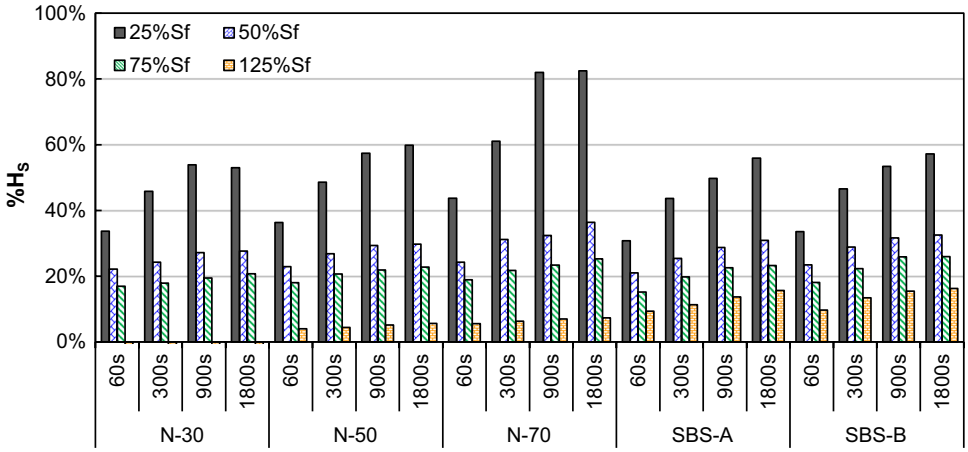

Fig. 3 Healing percentages under different damage levels and rest periods

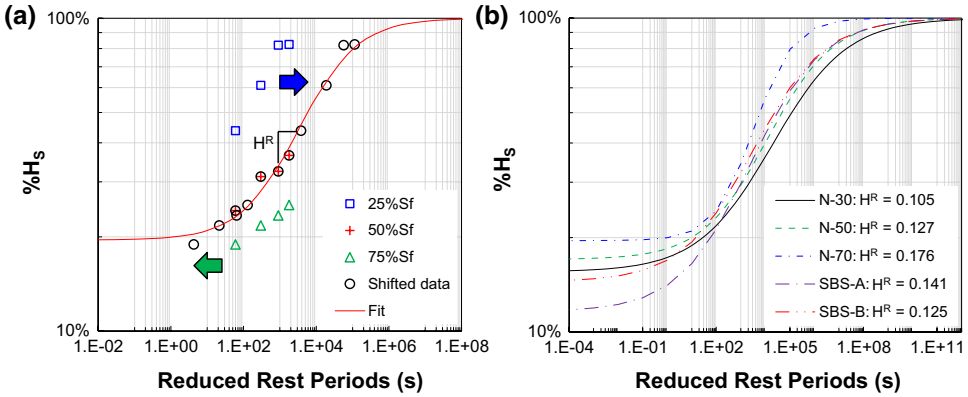

Fig. 4 Healing master curves: **a** construction via horizontal shifting and **b** results of the asphalt binders including the healing rates

as shown in Fig. 4a. Note that only the data for damage levels below fatigue failure S_f were employed in this process; once beyond failure, the VECD theory is no longer applicable due to the presence of macrocracks, which invalidates the premise of a continuum. By selecting 50% S_f as the reference damage level, all data points of different damage levels were shifted horizontally to form a master curve. The horizontal axis was then renamed as reduced rest period, which combined the physical rest period and damage level. As healing generally occurs with an upper asymptote of 100% in terms of $\%H_S$ and a lower positive asymptote, a sigmoidal function was utilized to fit the data points in the space of $\%H_S$ versus reduced rest period. Healing rate, as an index representing the overall healing potential, was then identified as the maximum slope of the fitted curve [12, 13]; see Fig. 4a. Figure 4b provides the healing master curves established for the five asphalt binders. As expected from $\%H_S$ shown in Fig. 3, the N-70 asphalt binder presented a master curve that lied above those of the remaining materials. The obtained H^R values are also included in Fig. 4b as part of the legend. It is seen that for both the neat and SBS-modified asphalt binders, a higher penetration (Table 1) corresponded to a higher healing rate; that is, softer binders tended to heal at a faster rate. The same trend has been reported by Lv et al. [3] and Sun et al. [8] despite different healing characterization approaches. The H^R parameter was used to investigate the implications of chemical characteristics on asphalt binder healing, as provided in the following section.

4 Chemical characteristics and correlation with healing

This section presents the chemical evaluation results in terms of fractionations using SARA and GPC approaches and averaged molecular structures via NMR, followed by their relationships explored with respect to the healing potential of the asphalt binders.

4.1 SARA fractions

The SARA fractionation result is given in Fig. 5a. For the neat asphalt binders, increase in the penetration from N-30 to N-70 corresponded to reduced asphaltenes percentages along with higher concentrations of the light and less polar fractions (saturates and aromatics). Similarly, within the modified group, the higher modification dosage used in SBS-B with slightly lower penetration corresponded to a higher concentration of asphaltenes and a lower percentage of the light fractions. To investigate the implications of SARA results on the healing potential of asphalt binders, a number of indices based on the four fractions, including the S/Ar ratio and the colloidal index [9, 26] were attempted. It was found that the total percentage of saturates and aromatics presented the best correlation with the healing rate H^R; see Fig. 5b. For both the neat and SBS-modified asphalt binders, a consistent trend of increasing healing potential with higher concentrations of the light fractions was noted. Based on the existing understanding [6, 10], these smaller and less polar molecules have higher mobility than the other fractions, which would facilitate the long-term molecular diffusion process and thus promote the macroscale healing.

4.2 Molecular weight distribution

Figure 6a provides the chromatogram of the five asphalt binders from the GPC analysis. It is seen that the three neat asphalt binders produced clearly separated curves, whereas the two modified binders yielded almost identical profiles due to the marginal difference in the SBS dosage. By dividing the chromatographic profile into three slices, the parameters namely LMS, MMS, and SMS were obtained. Despite the difference in the chromatogram as shown in Fig. 6a, the three-slice partition results for the five asphalt binders that did not differ substantially. The LMS of the neat binders were slightly higher than those of the SBS-modified asphalts by less than 2.6%, whereas the MMS of all five materials were between 68.8 and 70.8%. The concentration of small molecules, SMS, presented the best correlation with the

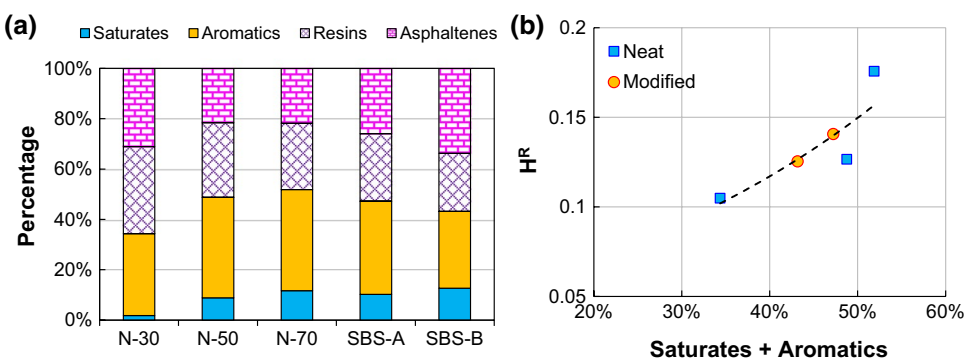

Fig. 5 SARA analysis: **a** fractionation result and **b** relationship between the light/low-polarity fractions (saturates and aromatics) and healing rate

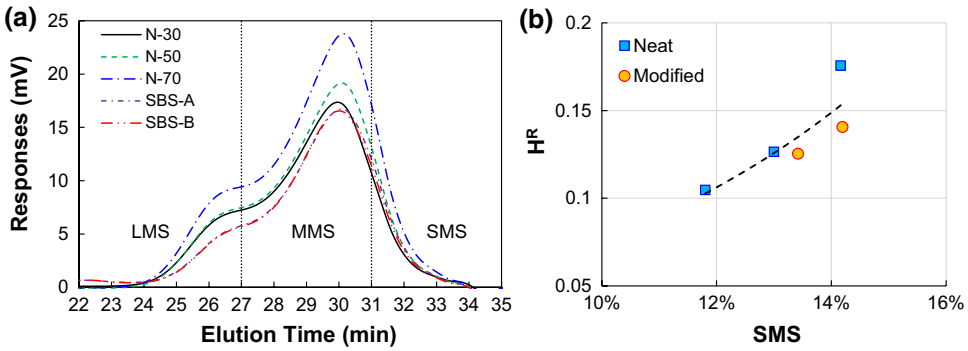

Fig. 6 GPC analysis: **a** chromatographic profiles and **b** relationship between the small molecule percentage and healing rate

healing rate H^R, as shown in Fig. 6b, in which a higher SMS corresponded to a faster healing rate. Presence of more small molecules appeared to enhance the healing process, which is essentially consistent with the relationship between the SARA light fractions and H^R as shown previously in Fig. 5b. Note that a direct correspondence between the SARA light fractions and GPC SMS is in general not available, since these two fractionation approaches are based on different properties of the molecules (chemical solubility versus hydrodynamic volume).

4.3 Molecular structure

Figure 7a–e presents the ^{1}H NMR spectra of the five asphalt binders in terms of the signal intensity versus chemical shift δ expressed in parts per million (ppm). The resonance singlet showing up at 0 ppm is the chemical shift reference of tetramethylsilane (TMS). The chemical shift of each characteristic peak represents a specific chemical environment of hydrogens. As shown in Fig. 7f, the shifts with δ between 6.0 and 9.0 ppm correspond to aromatic hydrogens, while those between 0 and 4.0 ppm are aliphatic hydrogens. The aliphatic region can be further separated into three parts: H_α (2.0–4.0 ppm) for hydrogens attached to a saturated carbons in the α-position relative to an aromatic ring, H_β (1.0–2.0 ppm) for hydrogens attached to paraffinic methylene carbons in the β-position or beyond relative to an aromatic ring, and H_γ (0.5–1.0 ppm) for hydrogens attached to paraffinic methyl carbons in the γ-position or farther with respect to an aromatic ring [27, 28].

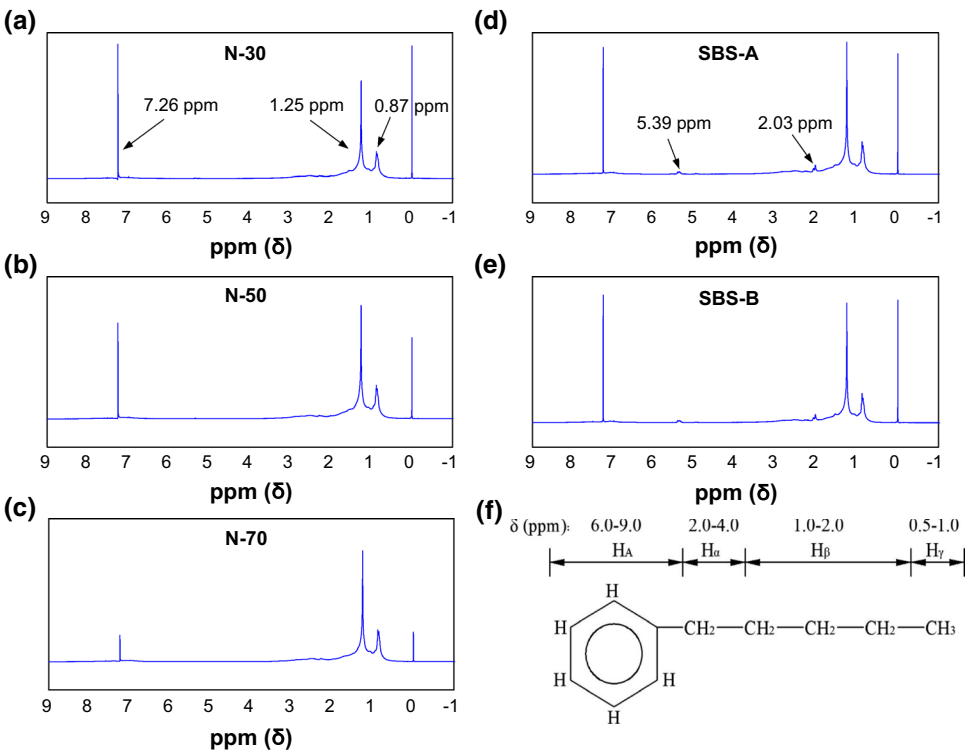

Fig. 7 ^{1}H NMR spectrum: **a**–**e** results for the five asphalt binders and **f** hydrogen molecules in the spectrum

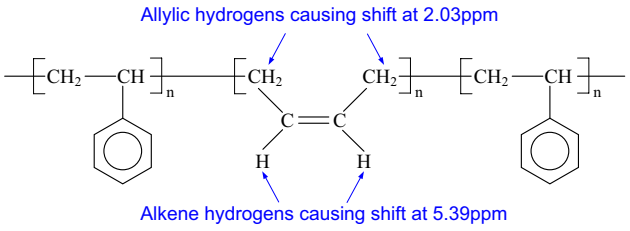

Fig. 8 Molecular structure of the SBS modifier

Table 3 Percentages of the various hydrogen types determined from NMR spectra

Asphalt binders	H_A (%)	H_α (%)	H_β (%)	H_γ (%)
N-30	6.9	15.1	57.4	20.6
N-50	5.1	14.5	59.2	21.2
N-70	2.5	13.7	61.0	22.8
SBS-A	9.6	17.2	54.6	18.6
SBS-B	10.2	17.6	54.6	17.6

As shown in Fig. 7a–c, the three neat binders exhibited qualitatively the same ^{1}H spectra, characterized by three resonance peaks at around 7.26, 1.25, and 0.87 ppm. The narrow spike at 7.26 ppm arose from aromatic hydrogens and was the major contributor to H_A (6.0–9.0 ppm). The two peaks at 1.25 and 0.87 ppm were relatively wider and originated from methylene and methyl hydrogens, contributing to H_β and H_γ, respectively. The shallow hump lying roughly between 2.0 and 3.0 ppm resulted from hydrogens attached to the α-carbons of the aromatic ring. The two SBS-modified binders presented very similar spectra as compared to the neat asphalts, except for the two tiny peaks at around 5.39 and 2.03 ppm. The chemical shift at 5.39 ppm did not belong to either group of aromatic and aliphatic hydrogens [29]; it was due to the presence of alkene protons (hydrogens attached to unsaturated carbons C=C) brought about by the SBS modifier, Fig. 8. The peak at 2.03 ppm was attributed to the allylic hydrogens (attached to the carbons which was in turn bonded to C=C) within the SBS molecules. Based on the above observations, it can be concluded that both the neat and SBS-modified binders were mainly comprised of hydrocarbon molecules characterized by aromatic rings and paraffinic chains and that the SBS modifier was primarily responsible for the presence of the unsaturated alkene groups.

Further quantification of the percentages of various hydrogen molecules utilized the ratio of the respective band areas to the whole spectrum area and the result is given in Table 3. Within the three neat asphalt binders, a higher penetration corresponded to considerably less aromatic rings in the molecular structure, which was accompanied with decreasing H_α and increasing H_β and H_γ. With introduction of SBS and increase in its dosage, H_A and H_α increased due to the added aromatic ring structures, while H_γ reduced as a result of the absence of the methyl hydrogens in the SBS molecules. Meanwhile, the two modified binders presented lower H_β than the neat asphalts, since every aromatic ring is associated with only one β-carbon in the SBS molecules, but typically with much more β-carbons in the asphalt molecules.

To investigate the effect of molecular structure on the self-healing property of the asphalt binders, the relationships between the healing index H^R and the percentages of the various hydrogen types were plotted as shown in Fig. 9. It is seen that for both the neat and SBS-modified binders, increase in H_A and H_α was associated with decreasing healing potential and H_γ was positively related with the healing rate. A higher H_β corresponded to a higher healing rate for the neat samples, but this parameter was almost identical between the two SBS-modified binders. The above relationships suggested that the asphalt systems with less ring structures, and thus more aliphatic chains tended to heal faster. This observation is essentially in agreement with the previous findings based on the use of S/Ar [9] and the ratio of methylene to methyl [10]. The hypothetical interpretation is that while the long aliphatic chains present small hindrance during molecular diffusion, they also act as little buffers hindering agglomeration of the polar fractions, thereby rendering a more dispersed structure that is beneficial for molecular diffusion [9–11].

It is also noted from Fig. 9 that based on any of the four hydrogen types, the SBS-modified binders did not fit in the trends for the neat asphalts. For example, according to Fig. 9a, the modified binders exhibited much higher healing potential than would be expected given their higher H_A values based on the relationship of H^R versus H_A for the neat asphalts. This observation underlined the complexity in molecular structures introduced by polymer modifier as related to asphalt binder self-healing. A parameter combining all or fewer of the four NMR parameters with the attempt to unify both the neat and modified binders was explored, but with no success.

5 Summary and conclusions

This study evaluated the healing potential of five neat and SBS-modified asphalt binders using the LASH test and assessed the chemical characteristics via the techniques of SARA fractionation, GPC, and NMR. The objective was to explore the relationships between the healing potential and molecular properties in terms of composition and structures. The following conclusions were drawn based on the findings:

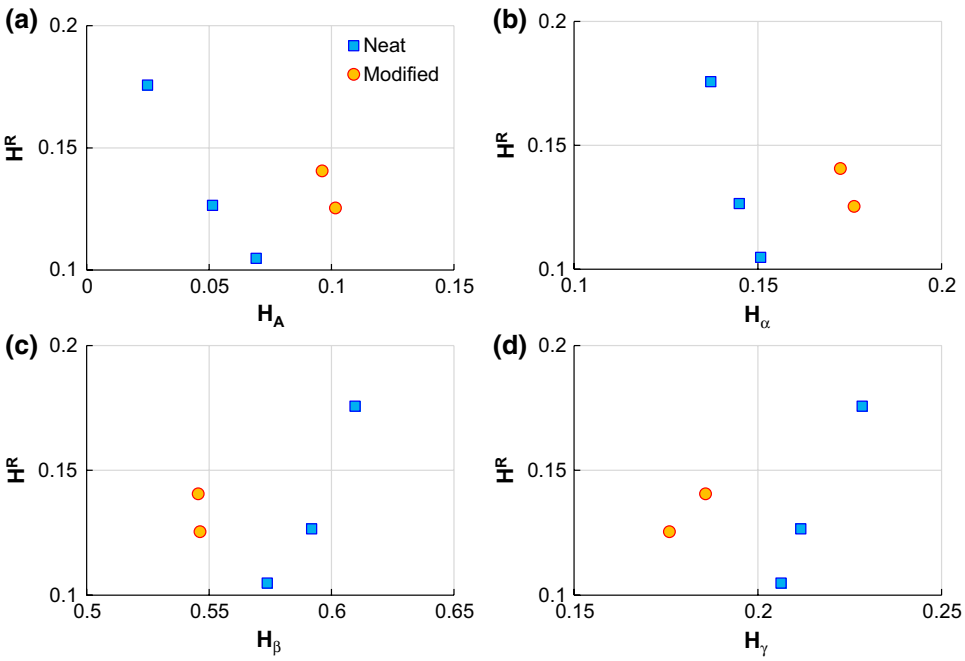

Fig. 9 Relationship between different hydrogen types and healing rate

- The LASH test proved to be an effective tool for healing characterization by constructing the healing master curves and obtaining the healing rate parameter. Within the neat asphalt binders, softer materials with higher penetrations presented a higher healing rate. The SBS-modified binders yielded healing rates that were within the range of the neat asphalts, and the polymer modifier appeared to retard crack propagation after fatigue failure.
- According to the SARA analysis, asphalt binders with higher penetrations contained higher percentages of light/low-polarity fractions of saturates and aromatics and tended to heal at a faster rate, which was attributed to the high mobility of these molecules that expected to facilitate the diffusion process across crack interfaces.
- The percentage of small molecules determined from GPC chromatogram was positively correlated with the healing rate for both the neat and modified asphalt binders, which suggested that the presence of more small molecules would promote self-healing.
- The distributions of hydrogen molecules according to ^{1}H NMR spectra were similar for the five asphalt binders. For both the neat and modified binders, the lower percentages of aromatic rings and more aliphatic chains were associated with higher healing rates. The understanding is that the presence of more aliphatic chains contributed to a well-dispersed material system that was more favorable to the molecular diffusion process. The SBS polymer modifier increased the concentration of aromatic rings in the asphalt system, but still yielded much higher healing potential than would be expected for the neat asphalts with the same H_A values.

The LASH and NMR tests revealed the complexity of SBS-modified asphalt binders in the self-healing and molecular structure properties. The LASH data suggested that the polymer modifier may retard the crack propagation more effectively than crack initiation. This finding necessitates the development of a fracture mechanics-based methodology for a more comprehensive consideration of the effect of SBS. The NMR results demonstrated the difference between the molecular structures of the asphalt cement and polymer modifier and that the modified binders need to be treated separately from the neat asphalts with respect to self-healing, unless a unifying molecular structural parameter can be identified.

Acknowledgements The authors would like to gratefully acknowledge the sponsorship from National Natural Science Foundation of China (51608018), Beijing Municipal Education Commission (KM201810005020) and Beijing Natural Science Foundation (8174059).

Compliance with ethical standards

Conflict of interest All authors declare that they have no conflict of interest.

Ethical approval This manuscript in part or in full has not been submitted or published anywhere and will not be submitted elsewhere until the editorial process is completed. The manuscript as well as the order of authorship has been approved by all the named authors.

References

1. Mogawer WS, Austerman A, Roque R, Underwood BS, Mohammad L, Zou J. Ageing and rejuvenators: evaluating their impact on high RAP mixtures fatigue cracking characteristics using advanced mechanistic models and testing methods. Road Mater Pavement Des. 2015;16(s2):1–28.
2. Cao W, Mohammad LN, Barghabany P, Cooper SBIII, Salari S. Comparison of asphalt mixtures crack resistance at intermediate temperatures using advanced test methods and theories. Transp Res Rec. 2018;2672(28):416–25.
3. Lv Q, Huang W, Zhu X, Xiao F. On the investigation of self-healing behavior of bitumen and its influencing factors. Mater Des. 2017;117:7–17.
4. Carpenter SH, Ghuzlan KA, Shen S. Fatigue endurance limit for highway and airport pavements. Transp Res Rec. 2003;1832:131–8.
5. Wool RP, O'Connor KM. A theory of crack healing in polymers. J Appl Phys. 1981;52(10):5953–63.
6. Bhasin A, Little DN, Bommavaram R, Vasconcelos K. A framework to quantify the effect of healing in bituminous materials using material properties. Road Mater Pavement Des. 2008;9(s1):219–42.
7. Bommavaram R, Bhasin A, Little DN. Determining intrinsic healing properties of asphalt binders. Transp Res Rec. 2009;2126:47–54.
8. Sun D, Yu F, Li L, Lin T, Zhu XY. Effect of chemical composition and structure of asphalt binders on self-healing. Constr Build Mater. 2017;133:495–501.
9. Santagata E, Baglieri O, Dalmazzo D, Tsantilis L. Rheological and chemical investigation on the damage and healing properties of bituminous binders. J Assoc Asph Paving Technol. 2009;78:567–96.
10. Kim YR, Little DN, Benson FC. Chemical and mechanical evaluation of healing mechanism of asphalt concrete. J Assoc Asph Paving Technol. 1990;59:240–75.
11. Little DN, Lytton RL, Williams D, Kim YR. Propagation and healing of microcracks in asphalt concrete and their contributions to fatigue. In: Usmani AM, editor. Asphalt science and technology. Boca Raton: CRC Press; 1997. p. 149–96.
12. Xie W, Castorena C, Wang C, Kim YR. A framework to characterize the healing potential of asphalt binder using the linear amplitude sweep test. Constr Build Mater. 2017;154:771–9.
13. Wang C, Xie W, Underwood BS. Fatigue and healing performance assessment of asphalt binder from rheological and chemical characteristics. Mater Struct. 2018;51:171.
14. AASHTO. Standard method of test for effect of heat and air on a moving film of asphalt binder (rolling thin-film oven test). Washington, DC: AASHTO T 240-13; 2017.
15. AASHTO. Standard method of test for estimating damage tolerance of asphalt binders using the linear amplitude sweep. Washington, DC: AASHTO TP 101-12; 2018.
16. Daly WH. Relationship between chemical makeup of binders and engineering performance: a synthesis of highway practice. Washington, DC: NCHRP Synthesis 511, Transportation Research Board; 2017.
17. Weigel S, Stephan D. Modelling of rheological and ageing properties of bitumen based on its chemical structure. Mater Struct. 2017;50:83.
18. ASTM. Standard test method for separation of asphalt into four fractions. West Conshohocken: ASTM D4124; 2009.
19. Jennings PW, Pribanic JAS, Dawson KR, Bricca CE. Use of HPLC and NMR spectroscopy to characterize asphaltic materials. Am Chem Soc Div Pet Chem. 1981;26(4):915–22.
20. Wahhab HIA, Asi IM, Ali FM, Al-Dubabi IA. Prediction of asphalt rheological properties using HP-GPC. J Mater Civ Eng. 1999;11(1):6–14.
21. Hasan MU, Ali MF, Bukhari A. Structural characterization of Saudi Arabian heavy crude oil by NMR spectroscopy. Fuel. 1983;62(5):518–23.
22. Wang C, Castorena C, Zhang J, Kim YR. Unified failure criterion for asphalt binder under cyclic fatigue loading. Road Mater Pavement Des. 2015;16(s2):125–48.
23. Safaei F, Castorena C, Kim YR. Linking asphalt binder fatigue to asphalt mixture fatigue performance using viscoelastic continuum damage modeling. Mech Time Depend Mater. 2016;20:299–323.
24. Cao W, Wang C. A new comprehensive analysis framework for fatigue characterization of asphalt binder using the Linear Amplitude Sweep test. Constr Build Mater. 2018;171:1–12.
25. Little DN, Lytton RL, Williams D, Kim YR. An analysis of the mechanics of microdamage healing based on the application of micromechanics first principles of fracture and healing. J Assoc Asph Paving Technol. 1999;68:501–42.
26. Loeber L, Muller G, Morel J, Sutton O. Bitumen in colloid science: a chemical, structural and rheological approach. Fuel. 1998;77(13):1443–50.
27. Huang J. Characterization of asphalt fractions by NMR spectroscopy. Pet Sci Technol. 2010;28(6):618–24.
28. Rossi CO, Caputo P, De Luca G, Maiuolo L, Eskandarsefat S, Sangiorgi C. 1H-NMR spectroscopy: a possible approach to advanced bitumen characterization for industrial and paving applications. Appl Sci. 2018;8(2):229.
29. Fini EH, Kalberer EW, Shahbazi A, Basti M, You Z, Ozer H, Aurangzeb Q. Chemical characterization of biobinder from swine manure: sustainable modifier for asphalt binder. J Mater Civ Eng. 2011;23(11):1506–13.